JOURNAL OF MAGNETIC RESONANCE **126,** 149–153 (1997)
ARTICLE NO. MN971140

How to Reduce the Residual H_2O Signal in the PFG DQ Experiments Recorded with Only *z* Gradients

Claudio Dalvit* and Jean Marc Böhlen†

**Novartis Pharma AG, CH-4002 Basel, Switzerland; and †Spectrospin AG, CH-8117 Fällanden, Switzerland*

Received December 18, 1996

The observation of multiple-quantum coherence involving H_2O (*1, 2*) has spurred great interest. The past few years have been punctuated by several publications dealing with this subject (*3–15*). Some of these effects are related to the multiple-echoes phenomenon first described in ^{3}He (*16, 17*).

Recently, we have demonstrated experimentally that ^{1}H 2D and 3D pure absorption double-quantum (DQ or 2Q) experiments recorded with gradients tilted at the magic angle (MAGs) results in spectra with the almost complete suppression of the H_2O signal (*18*). Similar findings have been obtained for the DQ-filtered COSY experiments (*9, 12*). Furthermore, the use of MAGs in DQ experiments achieves multiple-solvent suppression and suppression of the signals originating from intermolecular DQ coherence between solvent and solute (*19*). MAGs inhibit the conversion of H_2O antiphase magnetization present at the beginning of the acquisition period to in-phase magnetization and thus to observable signal (*2, 7, 13*). The efficiency of the conversion is proportional to $(3\cos^2\theta - 1)$ where θ is the angle between the gradient direction and the static magnetic field direction. For $\theta = 54.7°$, i.e., the magic angle, the function has zero value.

It should be pointed out that, in DQ imaging, it was observed that the use of composite gradients (i.e., gradients applied in all three directions x, y, and z) improved the H_2O signal suppression (*20*). However, no calibration of the x, y, z gradients was carried out in order to find the magic-angle condition. The better performance of the composite gradients vs z gradients was ascribed to the diminished probability of unwanted H_2O signal being rephased by a spurious gradient during acquisition. The experimental behavior of the residual solvent signal in the function of θ (*19*) which correlates with the function $(3\cos^2\theta - 1)$ appears to be strong evidence that the suppression of the H_2O signal in high-resolution NMR PFG DQ experiments is due to the zeroing effect of the demagnetizing field for $\theta = 54.7°$.

The presence of H_2O DQ coherence during the evolution period is likely due to different mechanisms. McCoy and Warren (*1*) have shown that radiation damping (*21–24*) can create H_2O DQ coherence in some experiments. The coupling of the spins with the coil generates multiple-quantum coherence in a way similar to the bilinear scalar couplings (*1*). If radiation damping were small, it would be refocused at the end of the spin-echo period of a DQ experiment. However, the use of high-Q probes, the long multiple-quantum excitation period, and probably deviation from the ideal 180° pulse makes the refocusing incomplete. Recently, we have demonstrated how to suppress radiation damping during the acquisition period of a PFG DQ experiment recorded with detection pulses different from 90° (*25*).

We describe here a modified version of the pulse sequences for the 2D and 3D DQ experiments which achieves suppression of radiation damping during the preparation period. This is shown in Fig. 1 for the 90° echo–antiecho DQ experiment. Two very weak gradients of equal sign and

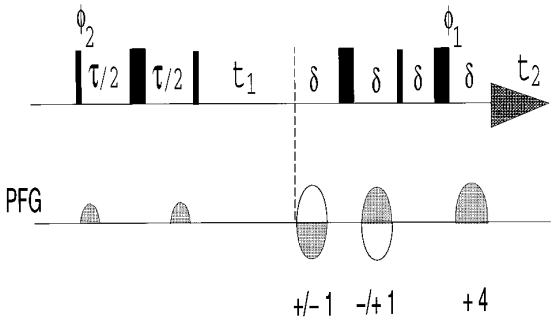

FIG. 1. Pulse sequence of the 2D 90° echo–antiecho PFG DQ experiment for the suppression of radiation damping during the excitation DQ period. The narrow and wide bars correspond respectively to 90° and 180° hard pulses. The phases are $\phi_1 = (x, -y, -x, y)$, $\phi_2 = 4(x), 4(-x)$, and $\phi_{rec} = 2(x, -x), 2(-x, x)$. All other pulses have phase x. The τ period is the DQ excitation period, and δ corresponds to the length of the gradient plus a recovery time. The first two gradients are weak PFGs applied at the beginning and end of the DQ excitation period, respectively. The last three gradients are used for the coherence-pathway selection. The strength of these last three gradients must obey the ratio +1:−1:+4 for the selection of one coherence pathway and −1:+1:+4 for the selection of the other coherence pathway. The data sets are then properly added. If triple-axis gradients are available, the last three gradients are magic angle gradients (MAGs) for efficient solvent suppression. The first two weak gradients can also be MAGs.

1090-7807/97 $25.00

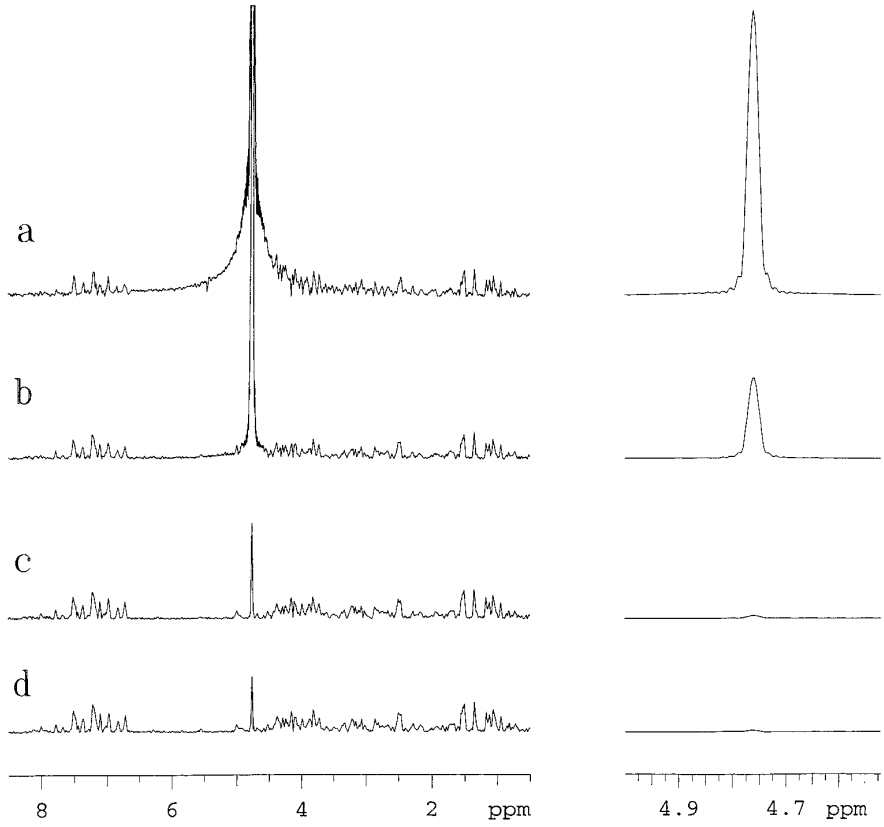

FIG. 2. One-dimensional spectra recorded with the basic pulse sequence of Fig. 1 for a 7 m*M* solution of the protein chicken egg-white lysozyme dissolved in 92% H_2O and 8% D_2O. The spectra have been recorded at T_e = 300 K with a Bruker DRX-600 spectrometer. The gradients were generated using a GREAT III unit connected to a 5 mm triple-resonance broadband inverse probe equipped with actively shielded *x*, *y*, *z*-gradient coils. The spectra are plotted at the same intensity level. The left side shows most of the spectrum, whereas the right side shows an expanded spectral region with reduced intensity centered at the H_2O chemical shift. The t_1 period was set to 10 ms, and only one coherence pathway was selected. Eight scans were recorded with acquisition time 122 ms and repetition time 2.122 s. The excitation DQ period τ was 30 ms long. The length of the sine-shaped gradients was 1.5 ms and the recovery time was 500 μs. The data were simply multiplied with a cosine-squared window function prior to Fourier transformation. The absolute value presentation is displayed. The spectra have been recorded without (a, c) and with (b, d) the first two weak *z* PFGs. The three coherence-selection gradients were *z* PFGs in (a, b) and MAGs in (c, d). The strength of the three MAGs in (c, d) was +16.2, −16.2 and +64.8% for the *x* and *y* components and +11.9, −11.9 and +47.6% for the *z* component. The strength of the three coherence-selection *z* PFGs in (a, b) was +20, −20 and +80%, whereas the strength of the first two *z* PFGs in (b, d) was +1%. The total strengths of the MAGs in (c, d) are equal to the strengths of the z PFGs in (a, b). The relative integral of the residual H_2O signal is about 40 (a), 10 (b), 1.1 (c), and 1 (d).

intensity are applied at the beginning and at the end of the DQ excitation period, respectively. The H_2O magnetization in this case remains completely defocused during the entire length of the spin-echo period and thus the radiation-damping effect is removed. Note that the two *z* gradients must be weak in order to minimize the effectiveness of the long-range part of the dipolar Hamiltonian in coherence transfer, according to Eq. 9 of Ref. (*5*). An alternative is the replacement of these two weak *z* gradients with two MAGs which suppress the effect of the demagnetizing field.

Figure 2 shows one-dimensional spectra recorded with the basic pulse sequence of Fig. 1 for a sample of the protein chicken egg-white lysozyme dissolved in H_2O. Only one of the two possible coherence pathways was selected with the gradients. The spectra in Figs. 2a and 2c have been recorded with only the three gradients for coherence selection, whereas the spectra in Figs. 2b and 2d have been recorded with the addition of two weak *z* PFGs located in the excitation double-quantum period. The residual H_2O signal is four times stronger in the experiment recorded with only 3 *z* PFGs (Fig. 2a) compared to the respective experiment recorded with 5 *z* PFGs (Fig. 2b). This is clearly experimental proof that some of the residual H_2O DQ signal observed in the DQ experiments originates from the radiation-damping mechanism acting in the preparation period. However, radiation damping cannot account for the total H_2O DQ signal present in the evolution period as shown by the residual signal in Fig. 2b. Other mechanisms such as the effect of long-range dipole–dipole interactions and violation of the high-temperature approximation may be responsible for the

remaining H_2O DQ signal. The use of MAGs for coherence selection results in excellent solvent suppression in both types of experiments as shown in Fig. 2c and Fig. 2d. Although the DQ signal present in t_1 is significant in the experiment lacking the first two weak PFGs, the use of MAGs efficiently suppresses this signal (Fig. 2c).

Two gradients have been implemented immediately before and after the 180° pulse of the DQ excitation period in DQ imaging (*20*). These act as a perfect EXORCYCLE (*26, 27*), assuring that only the magnetization inverted by the 180° pulse will be refocused. However, during the rest of the DQ excitation period, water magnetization is not defocused and thus radiation damping will be effective. This does not represent a problem in DQ imaging because radiation damping is very small, and consequently, both possible schemes for the first two PFGs would give similar results. However, differences are expected in high-resolution NMR DQ experiments recorded at high magnetic fields for biomolecules dissolved in H_2O. This can be appreciated in Fig. 3 which shows the residual H_2O signal present in the one-dimensional DQ spectra recorded with the basic pulse sequence of Fig. 1. The spectra have been recorded with only three coherence-selection *z* PFGs (Fig. 3a), and with the addition of two *z* PFGs located in the DQ excitation period (Figs. 3b, 3c). The two gradients were applied around the 180° pulse (Fig. 3b) and at the beginning and the end of the DQ excitation period (Fig. 3c). The relative integral of the residual H_2O signal in Fig. 3 is 13 (a), 6 (b), and 1 (c), thus showing that the best solvent suppression is achieved in the experiment where radiation damping is suppressed for the entire length of τ.

Note that the superior H_2O suppression in Fig. 3c is not due to the H_2O diffusion process occurring between the first and second gradient. This can be shown with a simple calculation. The signal intensity present at the end of the second refocusing PFG normalized to the signal intensity obtained in the absence of the two weak sine-shaped *z* PFGs is given by (*28*)

$$A = \exp[-\gamma^2 G^2 \delta^2 D(4\Delta - \delta)/\pi^2], \qquad [1]$$

where G and δ are the strength and duration of the two PFGs, respectively, Δ is the time between the start of the two PFGs, γ is the proton gyromagnetic ratio, and D is the translational diffusion coefficient of H_2O which at 25°C is 2.3×10^{-5} cm^2/s (*29*). With the parameters used for Fig. 2b and Fig. 3c, namely G about 0.5 G/cm, $\delta = 1.5$ ms, and $\Delta = 28$ ms, we obtain a value for A which is very close to unity, indicating that there is no H_2O-signal attenuation due to diffusion. This was also demonstrated experimentally. By tripling the strength of the first two *z* PFGs used for the spectra recorded in Fig. 2b and Fig. 3c, we did not obtain better solvent suppression. On the contrary, the spectra contained more H_2O residual signal, probably due to a more pronounced effect in coherence transferring of the long-range part of the dipolar Hamiltonian (data not shown). It should be pointed out that when the first two PFGs are made very strong, excellent H_2O suppression is again achieved. With strong PFGs, the effectiveness of the long-range part of the dipolar Hamiltonian in transferring coherence is approaching the zero value. Furthermore, the H_2O signal is reduced due to spatial diffusion occurring in the interval between the two PFGs. Although the signals of slowly diffusing macromolecules are not affected by the use of strong

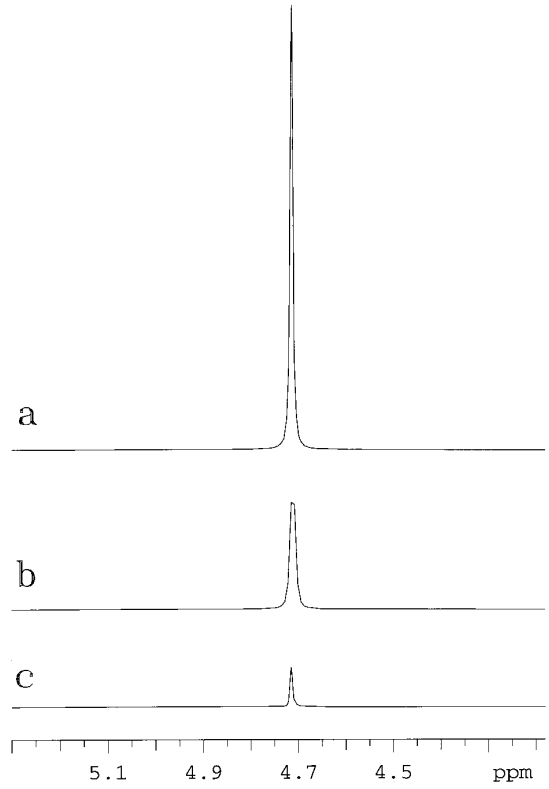

FIG. 3. One-dimensional spectra recorded with the basic pulse sequence of Fig. 1 for a 7 m*M* solution of the protein chicken egg-white lysozyme dissolved in 92% H_2O and 8% D_2O. The spectra have been recorded at T_e = 300 K using the same hardware described in the legend of Fig. 2. Only the spectral region centered at the H_2O chemical shift is displayed. The t_1 period was set to 10 ms and only one coherence pathway was selected. Eight scans were recorded with acquisition time 488 ms and repetition time 12.5 s. The excitation DQ period τ was 30 ms long. The length of the sine-shaped gradients was 1.5 ms and the recovery time was 500 μs. The data were multiplied with a cosine-squared window function prior to Fourier transformation. The absolute value presentation is displayed. The spectra are plotted at the same intensity level. The experiments have been recorded with only the three coherence-selection *z* PFGs (a) and with the addition of the two *z* PFGs applied close to the 180° pulse (b) and at the beginning and at the end of the DQ excitation period (c). The strength of the coherence selection *z* PFGs was +20, −20 and +80% in (a–c) and the strength of the first two *z* PFGs was +1% (b, c). The relative integral of the residual H_2O signal is 13 (a), 6 (b), and 1 (c).

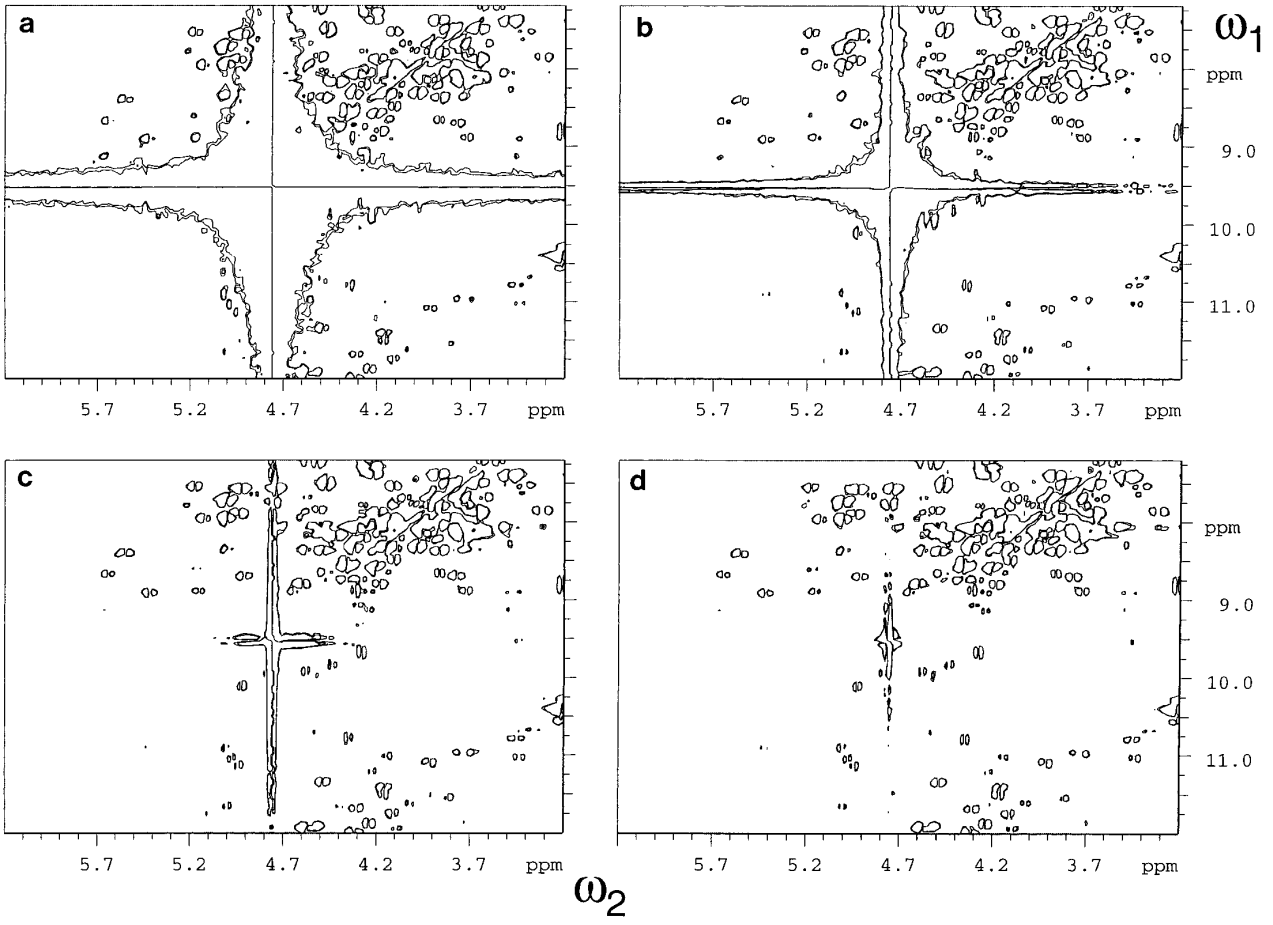

FIG. 4. Two-dimensional DQ spectra recorded with the basic pulse sequence of Fig. 1 for a 7 m*M* solution of the protein chicken egg-white lysozyme dissolved in 92% H_2O and 8% D_2O. A small region centered at $\omega_2 = \omega_{H_2O}$ and $\omega_1 = 2\omega_{H_2O}$ is displayed. Eight scans were recorded for each of the 512 t_1 increments (256 t_1 values for both the echo and anti-echo pathway selections). The experiments have been carried out at $T_e = 300$ K with the hardware described in the legend of Fig. 2. The ω_1 and ω_2 spectral widths were 12 and 15 ppm, respectively. The repetition time and τ were 1.5 s and 30 ms, respectively. The length of the sine-shaped gradients was 1.5 ms and the recovery time was 200 μs. The spectra have been recorded without (a, c) and with (b, d) the first two weak *z* PFGs. The three coherence-selection gradients were *z* PFGs in (a, b) and MAGs in (c, d). The strength of the three MAGs in (c, d) was ± 16.2, ∓ 16.2 and $+64.8\%$ for the *x* and *y* components and ± 11.9, ∓ 11.9 and $+47.6\%$ for the *z* component. The strength of the three coherence-selection *z* PFGs in (a, b) was ± 20, ∓ 20 and $+80\%$, whereas the strength of the first two *z* PFGs in (b, d) was $+1\%$. The total strengths of the MAGs in (c, d) are equal to the strengths of the *z* PFGs in (a, b). No treatment of the data was done for H_2O signal reduction. The weak H_2O residual signal in (d) allows the observation of several remote peaks at $\omega_2 = \omega^{\alpha}H$ and $\omega_1 = \omega^{N}H + \omega^{\beta}H$ which are almost degenerate with the H_2O signal.

gradients, the signals of small and medium-size molecules are partially attenuated.

The use of two weak additional gradients does not affect the intensity of the resonances of the molecules of interest as shown in Fig. 2. Therefore, we recommend the use of these two weak PFGs, as shown in Fig. 1, in all the 2D and 3D ^1H PFG DQ experiments developed up to now, especially when only *z* gradients are available.

Figure 4 shows an expanded spectral region centered at $\omega_2 = \omega_{H_2O}$ and $\omega_1 = 2\omega_{H_2O}$ of the 2D DQ spectra of lysozyme. The experiments have been acquired with the basic pulse sequence of Fig. 1. The spectra in Figs. 4a and 4c have been recorded with only the coherence-selection gradients, whereas the spectra in Figs. 4b and 4d have been recorded with the addition of the two weak *z* PFGs in the excitation DQ period. The results are similar to that observed in the 1D spectra. The spectrum recorded with 5 *z* PFGs (Fig. 4b) contains significantly less H_2O signal compared to the spectrum recorded with only 3 *z* PFGs (Fig. 4a). Note the remarkable H_2O suppression in the spectra recorded with MAGs (Figs. 4c, 4d). The spectra recorded with 3 MAGs and 2 *z* PFGs (Fig. 4d) have slightly better solvent suppression than the spectra recorded simply with 3 MAGs (Fig. 4c). Proton resonances close to the H_2O chemical shift are clearly visible in the spectra of Figs. 4c and 4d. The weak residual solvent signal has a lineshape which is dispersive

in both dimensions. The presence of this signal could be ascribed to different effects. One of these is the differential nonlinearity of the x, y, and z gradients (*30*) which results in deviation from the magic-angle condition for some part of the sample with consequent leakage of the H_2O signal. Due to the fact that the amount of antiphase H_2O magnetization present at the beginning of t_2 is larger in the DQ experiment recorded without the first two weak z PFGs, more H_2O magnetization will become observable via this mechanism. This explains the small differences in residual H_2O observed between Fig. 4c and Fig. 4d. It should be pointed out that the replacement of the first two weak z PFGs with two MAGs resulted in only marginal improvement of H_2O suppression compared to the spectra of Fig. 2d and Fig. 4d (data not shown). This is because the two z PFGs employed for the spectra of Fig. 2d and Fig. 4d are weak, and consequently, the effectiveness of the long-range part of the dipolar Hamiltonian in transferring coherence during the DQ excitation period is small.

In conclusion, we have shown that the radiation-damping mechanism acting in the double-quantum excitation period is responsible in part for the DQ H_2O signal present during the evolution period. The use of two weak PFGs applied at the beginning and end of the spin-echo period suppresses this mechanism. If z gradients are used, these should be strong enough to defocus the H_2O magnetization, but at the same time should be weak in order to minimize the effect of the long-range part of the dipolar Hamiltonian in transferring coherence. For proteins and other large macromolecules, the two PFGs can be made very strong in order to take advantage of the large difference in the self-diffusion coefficients of H_2O and proteins. However, the use of strong gradients will have the effect of reducing the intensity of the fast-exchanging NH resonances. We recommend the use of the two PFGs in the DQ excitation period of all the 2D and 3D ^1H PFG DQ experiments, in particular in the DQ experiments recorded with only z gradients.

REFERENCES

1. M. McCoy and W. S. Warren, *J. Chem. Phys.* **93,** 858 (1990).
2. R. Bowtell, R. M. Bowley, and P. Glover, *J. Magn. Reson.* **88,** 643 (1990).
3. D. Abergel, M. A. Delsuc, and J. Y. Lallemand, *J. Chem. Phys.* **96,** 1657 (1992).
4. W. S. Warren, Q. He, M. McCoy, and F. C. Spano, *J. Chem. Phys.* **96,** 1659 (1992).
5. W. S. Warren, W. Richter, A. H. Andreotti, and B. T. Farmer II, *Science* **262,** 2005 (1993).
6. J. Jeener, A. Vlassenbroek, and P. Broekaert, *J. Chem. Phys.* **103,** 1309 (1995).
7. W. Richter, S. Lee, W. S. Warren, and Q. He, *Science* **267,** 654 (1995).
8. G. J. Bowden, T. Heseltine, and M. J. Prandolini, *Chem. Phys. Lett.* **233,** 639 (1995).
9. P. C. M. Van Zijl, M. O. Johnson, S. Mori, and R. E. Hurd, *J. Magn. Reson. A* **113,** 265 (1995).
10. R. Bowtell and A. Peters, *J. Magn. Reson. A* **115,** 55 (1995).
11. M. Levitt, *Concepts Magn. Reson.* **8,** 77 (1996).
12. D. L. Mattiello, W. S. Warren, L. Müller, and B. T. Farmer II, *J. Am. Chem. Soc.* **118,** 3253 (1996).
13. S. Lee, W. Richter, S. Vathyam, and W. S. Warren, *J. Chem. Phys.* **105,** 874 (1996).
14. S. Vathyam, S. Lee, and W. S. Warren, *Science* **272,** 92 (1996).
15. P. Broekaert, A. Vlassebroek, J. Jeener, G. Lippens, and J. M. Wieruszeski, *J. Magn. Reson. A* **120,** 97 (1996).
16. G. Deville, M. Bernier, and J. M. Delrieux, *Phys. Rev. B* **19,** 5666 (1979).
17. D. Einzel, G. Eska, Y. Hirayoshi, T. Kopp, and P. Wölfle, *Phys. Rev. Lett.* **53,** 2312 (1984).
18. C. Dalvit and J. M. Böhlen, *J. Magn. Reson. B* **111,** 76 (1996).
19. C. Dalvit and J. M. Böhlen, *Magn. Reson. Chem.* **34,** 829 (1996).
20. R. E. Hurd, and D. M. Freeman, *Proc. Natl. Acad. Sci. USA* **86,** 4402 (1989).
21. A. Abragam, ''The Principles of Nuclear Magnetism,'' Oxford Univ. Press, London, 1961.
22. W. S. Warren, S. L. Hammes, and J. L. Bates, *J. Chem. Phys.* **91,** 5895 (1989).
23. D. Wu and C. S. Johnson, Jr., *J. Magn. Reson. A* **110,** 113 (1994).
24. H. Barjat, G. P. Chadwick, G. A. Morris, and A. G. Swanson, *J. Magn. Reson. A* **117,** 109 (1995).
25. C. Dalvit and J. M. Böhlen, *J. Magn. Reson. B* **113,** 195 (1996).
26. G. Bodenhausen, R. Freeman, and D. L. Turner, *J. Magn. Reson.* **27,** 511 (1977).
27. A. Bax and S. S. Pochapsky, *J. Magn. Reson.* **99,** 638 (1992).
28. E. O. Stejskal and J. E. Tanner, *J. Chem. Phys.* **42,** 288 (1965).
29. P. Stilbs, *Prog. NMR Spectrosc.* **19,** 1 (1987).
30. R. E. Hurd, A. Deese, M. O. Johnson, S. Sukumar, and P. C. M. Van Zijl, *J. Magn. Reson. A* **119,** 285 (1996).